

## Density and structure of undercooled liquid titanium

WANG HaiPeng, YANG ShangJing &amp; WEI BingBo\*

*Department of Applied Physics, Northwestern Polytechnical University, Xi'an 710072, China*

Received October 29, 2011; accepted December 16, 2011

For liquid Ti, it is difficult to achieve high undercooling because of its chemical reactivity; as a result, there is little information available on its properties and structure in the undercooled state. In this study, we investigate the density and structure, using molecular dynamics method, for the undercooling and superheating ranges 0–743 K and 0–457 K. The density increases quadratically for undercooling. At the melting temperature, the density is  $4.14 \text{ g/cm}^3$ , and first and second temperature coefficients are obtained. The pair correlation functions and coordination numbers indicate that the short range degree of order becomes increasingly significant with increasing undercooling.

**liquid metal, undercooling, density, liquid structure, titanium****Citation:** Wang H P, Yang S J, Wei B B. Density and structure of undercooled liquid titanium. *Chin Sci Bull*, 2012, 57: 719–723, doi: 10.1007/s11434-011-4945-6

In comparison with the majority of normal-state liquids, undercooled liquid metals display many unusual characteristics as a result of their thermodynamic metastability. This is particularly seen for metals with high melting-temperatures and these have attracted increasing research interest in the past ten years [1–6]. The densities and structures of metastable undercooled liquids are of great importance in understanding metastable liquid metals. However, little is known about the densities and structures of metastable liquid metals compared with those of stable liquids above the melting temperatures.

Ti is widely used in various applications such as airframes and turbine blades because it has excellent properties, including excellent strength, low density, good ductility, and superior resistance to chemical processes. However, its melting temperature is very high, at 1943 K, which is especially for high reactivity in the liquid state. These factors cause great difficulties in the experimental determination of the properties of liquid Ti. Accordingly, information on the density and liquid structure is scarce. The requirement for this information is increasing as a result of the extensive application of Ti in various industrial alloys.

In the past ten years, several researchers have reported

densities of liquid Ti. Rhim et al. [7] measured the density of liquid Ti in the temperature range 1650–2000 K using an electrostatic levitator (ESL). Paradis et al. [8] obtained the density of liquid Ti using an ESL method in the temperature range 1750–2050 K. Ishikawa et al. [9] also reported the density obtained using their ESL facility in the temperature range 1680–2060 K. However, there are some discrepancies among these reported results. Detailed investigations of the densities are still needed and the temperature regimes studied so far have not been broad enough. In order to further understand the physical characteristics of liquid Ti, density changes and liquid structures are required over a broad temperature range, especially for the metastable undercooled regime.

The liquid structure is also of importance in studies of undercooled liquid Ti. However, it is extremely difficult to obtain detailed structural information because of its metastable characteristics and rapid atom diffusion. Recently, an experimental investigation of the liquid structures of metals was performed by combining containerless processing with X-ray scattering, synchrotron X-ray diffraction, and neutron diffraction methods [10–13]. For liquid Ti, Lee et al. [14] measured the structure factor of an electrostatically levitated Ti droplet at 282 K undercooling by synchrotron X-ray diffraction, and Holland-Moritz et al. [15] determined the

\*Corresponding author (email: [bbwei@nwpu.edu.cn](mailto:bbwei@nwpu.edu.cn))

structure factor of liquid Ti at about 200 K undercooling by neutron scattering combined with an electromagnetic levitation technique. However, many problems with respect to the density and structure of liquid Ti still need to be resolved.

Molecular dynamics method, combining with a reasonable potential model, has been used to simulate the properties and liquid structures of undercooled metals [16–19]. Compared with experimental studies, high undercooling is easily achieved in simulations, and more detailed information can therefore be accordingly obtained. The objective of the present work is to study the density and structure of metastable undercooled Ti over a much broader temperature range than those previously studied. Subsequently, the molar volume and thermal expansion coefficient are also derived.

## 1 Materials and method

Selection of the potential model is very important for the final calculated results. In density functional theory, the modified embedded atom method (MEAM) was proposed by Baskes, based on the potential model of an embedded atom method [20]. As well as describing metals with cubic structure, the MEAM model can also deal with metals with hexagonal structures, including Ti [21,22]. The MEAM potential model is expressed by [20]

$$E_{\text{tot}} = \sum_i \left[ F_i(\rho_i) + \frac{1}{2} \sum_{i,j(i \neq j)} \phi_{ij}(r_{ij}) \right], \quad (1)$$

where  $F_i$  is the energy of the embedded atom  $i$  in an electron density  $\rho_i$ ,  $\phi_{ij}$  is a pair of potential interactions between atoms  $i$  and  $j$ , which is summed over all neighbors  $j$  of atom  $i$  within the cutoff distance.

In the present work, 32000 Ti atoms are arranged in a cubic box as the liquid structure. The system is subjected to periodic boundary conditions in three dimensions under constant pressure and constant temperature. The time step is 1 fs and the pressure is set to  $10^5$  Pa. The temperature is adjusted every 50 steps. It starts at 3000 K to obtain an equilibrium liquid state. The initial temperature is kept constant for 200000 steps. The cooling process, with a cooling rate of  $10^{13}$  K/s, is performed for calculations at 100 K temperature intervals. At each temperature, 100000 steps are carried out for equilibrium. The last 50000 steps are used to calculate the final results. During the calculations, the system is kept in a liquid state by monitoring the pair-distribution function (PDF) and the mean-square displacement versus the simulated time. All codes are run in a Lenovo 1800 Cluster system.

## 2 Results and discussion

Density data play a fundamental role in numerical modeling

and materials design. The density of liquid Ti is calculated as a function of temperature, as illustrated in Figure 1. The density  $\rho$  exhibits a nonlinear dependence on the temperature  $T$ :

$$\rho = 4.14 - 2.15 \times 10^{-4}(T - T_m) - 3.71 \times 10^{-8}(T - T_m)^2 \text{ (g/cm}^3\text{)}, \quad (2)$$

where the melting point  $T_m$  is equal to 1943 K. The calculated temperature for the density of liquid Ti is in the range 1200–2400 K, including 743 K undercooling and 457 K superheating. Such a large undercooling is hard to achieve experimentally. From eq. (2), the density at the melting temperature is  $4.14 \text{ g/cm}^3$ , and its first and second temperature coefficients are  $-2.15 \times 10^{-4} \text{ g cm}^{-3} \text{ K}^{-1}$  and  $-3.71 \times 10^{-8} \text{ g cm}^{-3} \text{ K}^{-2}$ .

Figure 1 also presents the density results for liquid Ti obtained by other researchers, for evaluation of the present results obtained by molecular dynamics methods. Rhim et al. [7] measured the density of liquid Ti in the temperature range 1650–2000 K using an ESL, and the following linear expression was obtained:

$$\rho = 4.208 - 5.08 \times 10^{-4}(T - T_m) \text{ (g/cm}^3\text{)}. \quad (3)$$

This result is also illustrated in Figure 1, and includes a maximum undercooling of 293 K, as marked by line 1. It can be seen that Rhim's result is larger than the present result. At the melting temperature, only a difference of  $0.07 \text{ g/cm}^3$  exists between the two results, i.e. Rhim's result of  $4.208 \text{ g/cm}^3$  is 1.6% larger than the present value of  $4.14 \text{ g/cm}^3$ . However, the present temperature coefficient is larger than that obtained by Rhim's experiments.

Paradis et al. [8] measured the density of liquid Ti using an ESL method and derived the following correlation:

$$\rho = 4.10 - 9.90 \times 10^{-4}(T - T_m) \text{ (g/cm}^3\text{)}, \quad (4)$$

where the experimental temperature range is 1750–2050 K, and includes a maximum undercooling of 193 K. The present calculated value of the density at the melting temperature is

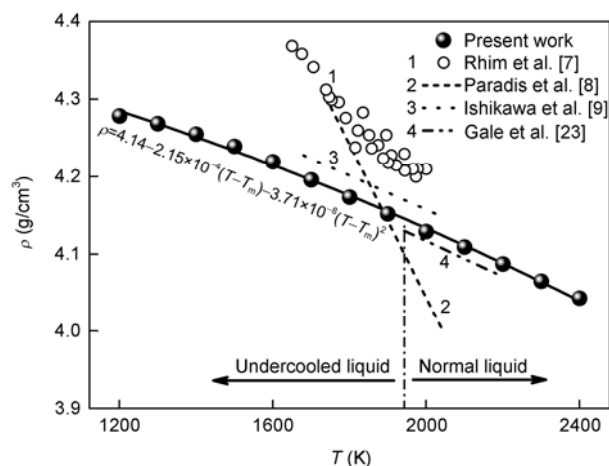


Figure 1 Density of liquid Ti versus temperature.

very close to Paradis's experimental result. However, there is a large difference between the two temperature coefficients.

Ishikawa et al. [9] also determined the density of liquid Ti using their ESL facility and derived the following relationship:

$$\rho = 4.17 - 2.2 \times 10^{-4} (T - T_m) \text{ (g/cm}^3\text{)}, \quad (5)$$

where the experimental temperature range is 1680–2060 K, and includes a maximum undercooling of 263 K.

The density of liquid Ti in Smithells Metals Reference Book [23] is

$$\rho = 4.13 - 2.3 \times 10^{-4} (T - T_m) \text{ (g/cm}^3\text{)}. \quad (6)$$

According to the above analysis, the maximum undercoolings achieved by Rhim, Paradis, and Ishikawa are 293, 193 and 263 K, respectively. In Smithells Metals Reference Book [23], only the data for the density of liquid Ti above the melting temperature are given. The four previously obtained densities at the melting temperature are as follows: Rhim's result is 4.208 g/cm<sup>3</sup>, Paradis's result is 4.10 g/cm<sup>3</sup>, Ishikawa's result is 4.17 g/cm<sup>3</sup>, and the result in [13] is 4.13 g/cm<sup>3</sup>. The present value is 4.14 g/cm<sup>3</sup>. Among these results, the maximum is Rhim's value of 4.208 g/cm<sup>3</sup>, the minimum value is Paradis's result of 4.10 g/cm<sup>3</sup>, and the difference between them is 0.108 g/cm<sup>3</sup>. Such a small difference is quite satisfactory.

However, there are large differences among the temperature coefficients reported by different researchers. Paradis's temperature coefficient,  $-9.9 \times 10^{-4} \text{ g cm}^{-3} \text{ K}^{-1}$ , is the minimum. The second lowest,  $-5.08 \times 10^{-4} \text{ g cm}^{-3} \text{ K}^{-1}$ , is Rhim's result, and the others are approximate. Although there are no significant differences among the density values at the melting temperature, the deviations among these results become increasingly large when the temperature deviates from the melting temperature for either the superheated state or the undercooled state. In terms of the above analysis, the present results agree well with Ishikawa's results (line 3) and the data in [13] (line 4). Accordingly, it can be concluded that our molecular dynamics simulation provides reasonable density data for liquid Ti, especially for a highly undercooled state.

According to the present density, important physical properties such as the molar volume and thermal expansion coefficient, which have close relationships with the density, could be derived for liquid Ti. The molar volume  $V_m$  of liquid Ti is computed and given in Figure 2 (hollow circles), and can be expressed by

$$V_m = 10.86 + 1.03 \times 10^{-4} T + 1.28 \times 10^{-7} T^2 \text{ (cm}^3\text{/mol)}. \quad (7)$$

Figure 2 shows that  $V_m$  increases nonlinearly with increasing temperature;  $V_m$  is 11.56 cm<sup>3</sup>/mol at the melting temperature of 1943 K, but  $V_m$  drops to 11.19 cm<sup>3</sup>/mol when the undercooling achieves 743 K. It is evident that the molar volume at the maximum undercooling is 3.3% smaller

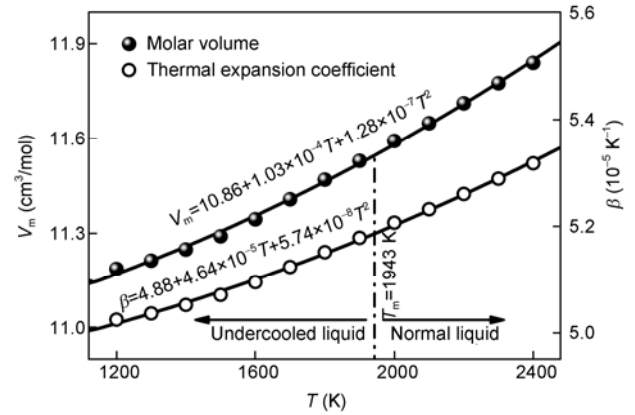


**Figure 2** Molar volume and thermal expansion coefficient of liquid Ti versus temperature.

than that at the melting point. For solid Ti,  $V_m$  is 10.64 cm<sup>3</sup>/mol at room temperature. This means that the value  $V_m$  for liquid Ti at 1943 K is 8.6% larger than that of solid Ti at 293 K. For the maximum undercooling of 768 K, the molar volume of liquid Ti is 5.2% larger than that of solid Ti at room temperature. This indicates that the structure of liquid Ti may change accordingly.

The thermal expansion coefficient  $\beta$  can be expressed as

$$\beta = -\rho^{-1} \frac{\partial \rho}{\partial T}. \quad (8)$$

Based on the above equations and the density results, the thermal expansion coefficients of liquid Ti are computed and shown in Figure 2; they can be expressed as

$$\beta = 4.88 + 4.64 \times 10^{-5} T + 5.74 \times 10^{-8} T^2. \quad (9)$$

The thermal expansion coefficient increases nonlinearly with increasing temperature coefficient. The thermal expansion coefficients of liquid Ti are of the order of magnitude  $10^{-5}$ . However, those of solid Ti are of the order of magnitude  $10^{-6}$ ; for example,  $\beta$  at 373 K is  $8.8 \times 10^{-6} \text{ K}^{-1}$ , and  $\beta$  at 1073 K is  $9.9 \times 10^{-6} \text{ K}^{-1}$ . It can be seen that  $\beta$  for Ti in the liquid state is much larger than that of solid; this may be because the inter-atomic forces in liquid metals are much weaker than those in solid metals.

Furthermore, the liquid structure of Ti can be represented by the PDF; this is computed using the equation  $g(r) = V \langle n_i(r, r + \Delta r) \rangle / (4\pi r^2 \Delta r N)$ , where  $V$  is the calculated cell volume,  $n_i(r, r + \Delta r)$  is the atom number around the  $i$ th atom in a spherical shell between  $r$  and  $r + \Delta r$ ,  $\langle \dots \rangle$  is the average symbol, and  $N$  is the atom number. This is calculated in the stable superheated state and metastable undercooled state for liquid Ti. For undercooled liquid Ti in particular, the undercooling is sufficiently large to enable the study of structural changes at the atomic scale. For clarity, only the PDFs at four temperatures, 2400 K (highly superheated state), 2000 K (near the melting temperature), 1600 K (undercooled state), and 1200 K (highly undercooled state) are

presented in Figure 3.

In Figure 3, clear peaks exist at the first-neighbor distance. With increasing distance, the PDF values approximate to 1. This suggests that the Ti atoms in the simulated system are ordered in the short range and disordered in the long range. These are typical characteristics of liquids. Although the four PDFs look similar to each other, there are still some differences among them. The first peak heights of the PDFs change significantly with temperature; this represents the degree of order of the Ti atoms at the first-neighbor distance. For the peaks at the sub-neighbor distance, a saddle occurs at 2400 K, the saddle changes to two small peaks at 2000 K, to two obvious peaks instead of a saddle at 1600 K, and three small peaks appear at 1200 K, indicating that the liquid structure of Ti changes when liquid Ti changes from a highly superheated state to a metastable undercooled state.

Figure 4 illustrates the PDF heights at the first- and sub-neighbor distances of liquid Ti. The PDF values at  $R_1$  (Figure 4(a)) decrease with increasing temperature. At 1200 K, the PDF at  $R_1$  is 4.95, which is 43% larger than the value of 3.47 at 2400 K. It is apparent that the degree of order of the atom distribution increases from the normal liquid to the undercooled liquid. The second peaks are also analyzed at different temperatures, and are shown in Figure 4(b). The features are similar to those of the PDFs at  $R_1$ , and the PDFs at  $R_2$  increase with increased undercooling. Comparing the PDF at  $R_2$  at 1200 K with that at 2400 K shows that the value is enhanced by 32% when liquid Ti cools from a superheated state at 2400 K to a highly undercooled state at 1200 K.

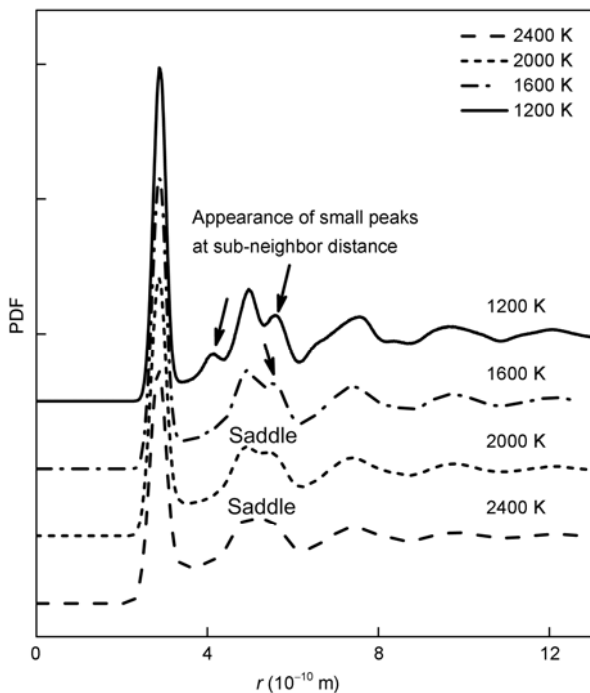


Figure 3 Pair distribution functions of liquid Ti versus temperature.

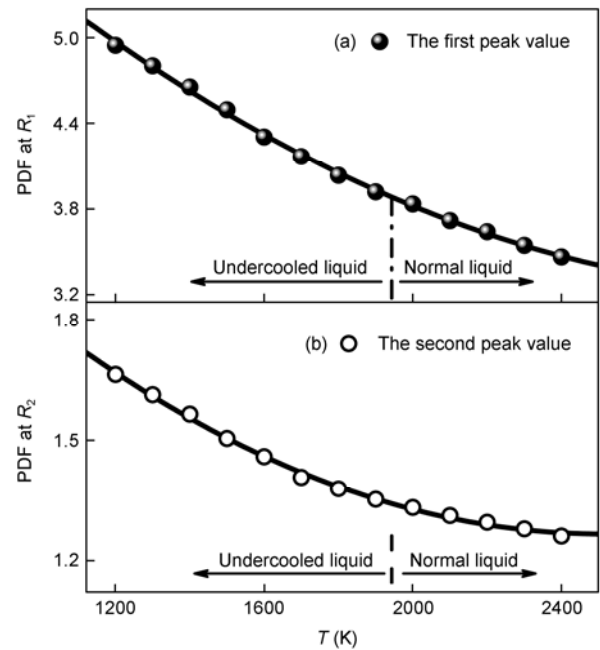


Figure 4 Pair distribution function heights at (a) first- and (b) sub-neighbor distances of liquid Ti versus temperature.

The coordination number of liquid Ti is also computed to analyze the liquid structure. First, the cutting distances  $r_c$  are determined from the first PDF peaks, as shown in Figure 5. It can be seen that  $r_c$  slightly increases with increasing temperature. The coordination number is almost independent of the temperature, and is in the range 10.0–10.3 from 1200 to 2400 K. This is different from the characteristics of the PDF peak heights.

### 3 Concluding remarks

In summary, the densities and structures of liquid Ti were investigated in the temperature range 1200–2400 K, including both superheated and undercooled states. The density

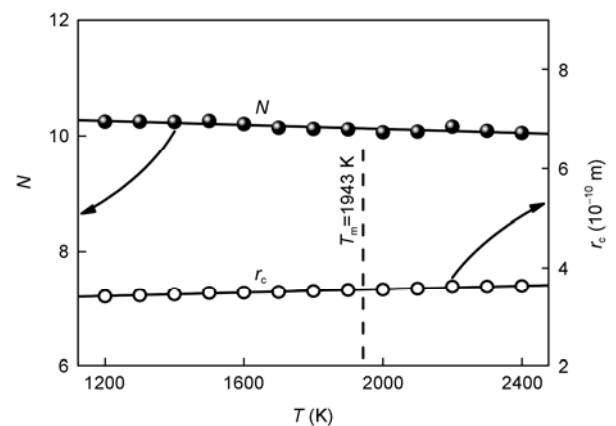


Figure 5 Coordination number and cutting distance of liquid Ti versus temperature.

increases nonlinearly with increased undercooling. At the melting temperature, the density is  $4.14 \text{ g/cm}^3$ , and its first and second temperature coefficients are  $-2.15 \times 10^{-4} \text{ g cm}^{-3} \text{ K}^{-1}$  and  $-3.71 \times 10^{-8} \text{ g cm}^{-3} \text{ K}^{-2}$ . The present work provides density values over a broader temperature range, especially for larger undercooling regimes, than those in previous studies. The maximum undercooling is 743 K. Such a large undercooling is hard to achieve experimentally. Based on the highly accurate calculated density, the molar volume and thermal expansion coefficient are derived; these increase quadratically with increasing temperature.

The PDF heights at the first-neighbor distance increase with decreasing temperature. For 1200 K, the PDF at  $R_1$  is 4.95, which is 43% larger than the value of 3.47 at 2400 K. The PDF at the sub-neighbor distance is similar to the PDF at  $R_1$ , which increases with increased undercooling. A comparison of the PDF at  $R_2$  at 1200 K with that at 2400 K shows that the value is enhanced by 32% when liquid Ti cools from a superheated state at 2400 K to a highly undercooled state at 1200 K. The above characteristics indicate that the degree of order of the atom distribution increases from the normal liquid to the undercooled liquid. However, the coordination number changes little, and remains in the range 10.0–10.3 from 1200 K to 2400 K.

*This work was supported by the National Natural Science Foundation of China (50971103 and 50971105), the Program for New Century Excellent Talents, the Natural Science Foundation of Shaanxi Province (2010JQ6004), the Shaanxi Project for Young New Star in Science and Technology and the NPU Foundation for Fundamental Research.*

- Shen Y T, Kim T H, Gangopadhyay A K, et al. Icosahedral order, frustration, and the glass transition: Evidence from time-dependent nucleation and supercooled liquid structure studies. *Phys Rev Lett*, 2009, 102: 057801
- Pietro Paolo A, Senesi R, Andreani C, et al. Excess of proton mean kinetic energy in supercooled water. *Phys Rev Lett*, 2008, 100: 127802
- Ganesh P, Widom M. Liquid-liquid transition in supercooled silicon determined by first-principles simulation. *Phys Rev Lett*, 2009, 102: 075701
- Luo B C, Wang H P, Wei B. Phase field simulation of monotectic transformation for liquid Ni-Cu-Pb alloys. *Chin Sci Bull*, 2009, 54: 183–188
- Hong Z Y, Lu Y J, Xie W J, et al. The liquid phase separation of Bi-Ga hypermonotectic alloy under acoustic levitation condition. *Chin Sci Bull*, 2007, 52: 1446–1450
- Wang H P, Chang J, Wei B. Measurement and calculation of surface tension for undercooled liquid nickel and its alloy. *J Appl Phys*, 2009, 106: 033506
- Paradis P F, Rhim W K. Non-contact measurements of thermophysical properties of titanium at high temperature. *J Chem Thermodyn*, 2000, 32: 123–133
- Paradis P F, Ishikawa T, Yoda S. Experiments in materials science on the ground and in reduced gravity using electrostatic levitators. *Adv Space Res*, 2008, 41: 2118–2125
- Ishikawa T, Paradis P F. Thermophysical properties of molten refractory metals measured by an electrostatic levitator. *J Electron Mater*, 2005, 34: 1526–1532
- Kordel T, Holland-Moritz D, Yang F, et al. Neutron scattering experiments on liquid droplets using electrostatic levitation. *Phys Rev B*, 2011, 83: 104205
- Kalay I, Kramer M J, Napolitano R E. High-accuracy X-ray diffraction analysis of phase evolution sequence during devitrification of  $\text{Cu}_{50}\text{Zr}_{50}$  metallic glass. *Metall Mater Trans A*, 2011, 42A: 1144–1153
- Higuchi K, Kimura K, Mizuno A, et al. Density and structure of undercooled molten silicon using synchrotron radiation combined with an electromagnetic levitation technique. *J Non-Cryst Solids*, 2007, 353: 2997–2999
- Kim T H, Lee G W, Sieve B, et al. *In situ* high-energy X-ray diffraction study of the local structure of supercooled liquid Si. *Phys Rev Lett*, 2005, 95: 085501
- Lee G W, Gangopadhyay A K, Kelton K F, et al. Difference in icosahedral short-range order in early and late transition metal liquids. *Phys Rev Lett*, 2004, 93: 037802
- Holland-Moritz D, Heinen O, Bellissent R, et al. Short-range order of stable and undercooled liquid titanium. *Mater Sci Eng A*, 2007, 449: 42–45
- Jakse N, Pasturel A. Dynamics of liquid and undercooled silicon: An *ab initio* molecular dynamics study. *Phys Rev B*, 2009, 79: 144206
- Gheribi A E. Molecular dynamics study of stable and undercooled liquid zirconium based on MEAM interatomic potential. *Mater Chem Phys*, 2009, 116: 489–496
- Morishita T. How does tetrahedral structure grow in liquid silicon upon supercooling. *Phys Rev Lett*, 2006, 97: 165502
- Wang H P, Chang J, Wei B. Density and related thermophysical properties of metastable liquid Ni-Cu-Fe ternary alloys. *Phys Lett A*, 2010, 374: 2489–2493
- Baskes M I. Modified embedded-atom potentials for cubic materials and impurities. *Phys Rev B*, 1992, 46: 2727–2742
- Zhang J M, Wang D D, Xu K W. Calculation of the surface energy of hcp metals by using the modified embedded atom method. *Appl Surf Sci*, 2006, 253: 2018–2024
- Kim Y M, Lee B J, Baskes M I. Modified embedded-atom method interatomic potentials for Ti and Zr. *Phys Rev B*, 2006, 74: 014101
- Gale W F, Totemeier T C. *Smithells' Metals Reference Book*. 8th ed. Burlington: Elsevier Butterworth Heinemann, 2004. 14–10

**Open Access** This article is distributed under the terms of the Creative Commons Attribution License which permits any use, distribution, and reproduction in any medium, provided the original author(s) and source are credited.